Supplementary Material for
R^3**LIVE++**: A **R**obust, **R**eal-time, **R**adiance Reconstruction Package with a Tightly-coupled **L**iDAR-**I**nertial-**V**isual State **E**stimator

Section 1: LiDAR- and Visual- challenging scenarios in NCLT-dataset.

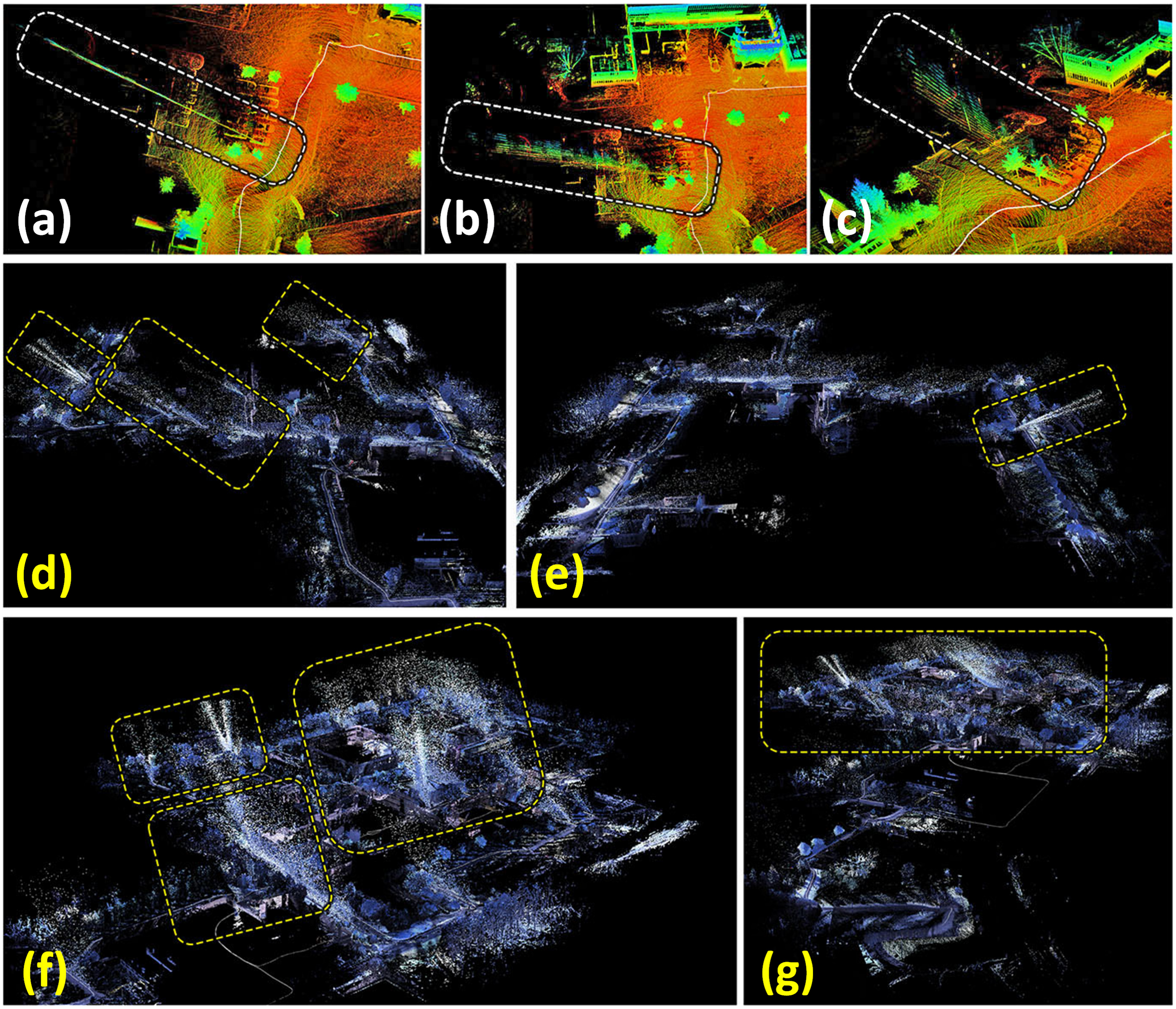

Fig. 1 – When facing the sun, LiDAR systems often exhibit a considerable number of noise points due to Sunlight contamination [1]. Sun contamination occurs when the laser beam emitted by the LiDAR sensor interacts with direct sunlight or reflections from shiny surfaces. In NCLT-dataset, we have observed a large number of sunlight induced noises. This type of noise can lead to the generation of misleading obstacles in the generated map, as illustrated in (a$\sim$c), consequently affecting the accuracy of LiDAR-based odometry systems for localization. When examining the NCLT sequences captured during the mid-noon period, we can observe a substantial amount of noise attributed to sunlight, as highlighted within the framebox in (d$\sim$g).

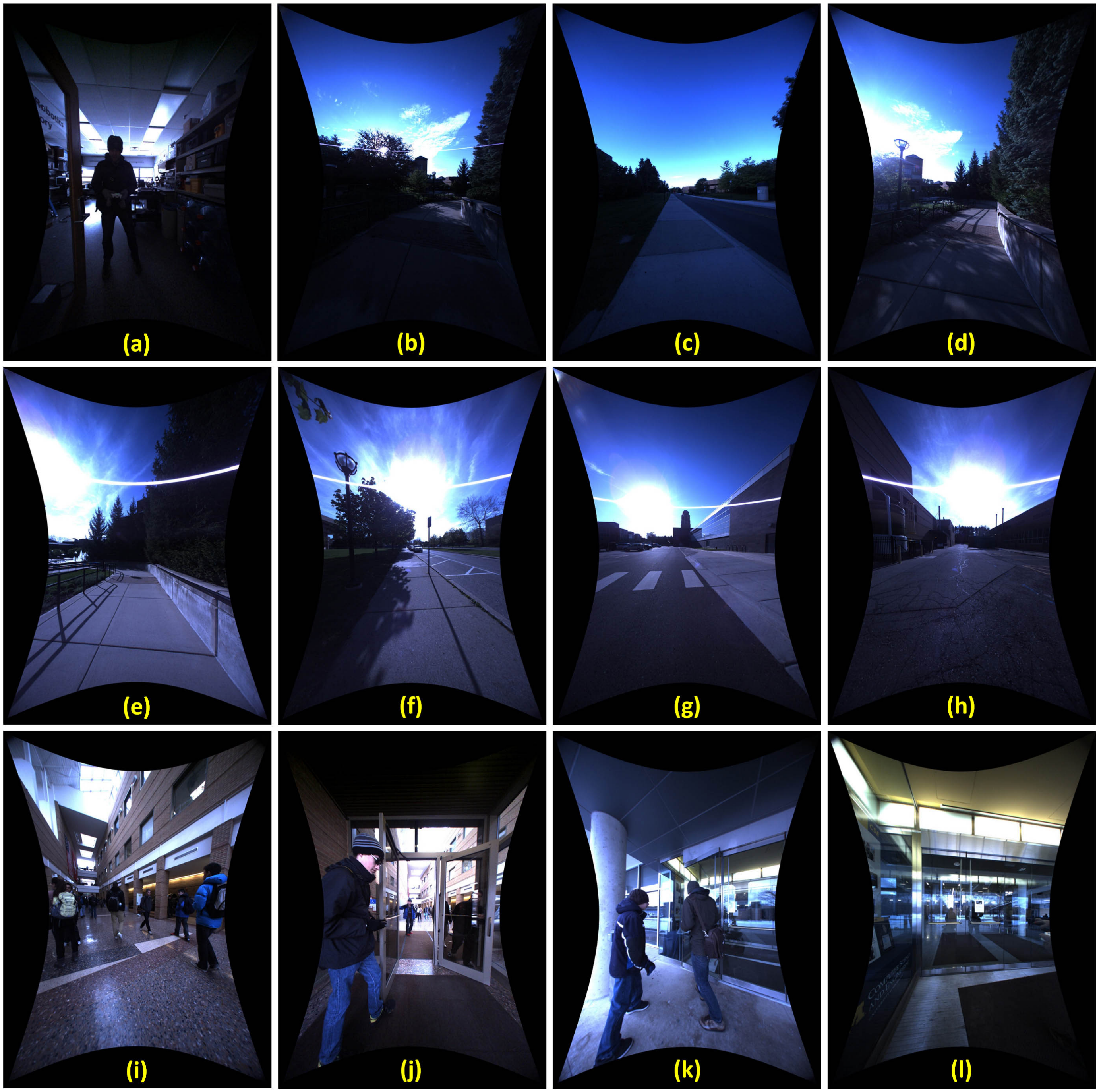

Fig. 2 – In NCLT-dateset, we have noticed a considerable number of images that are under-exposure (a∼d), over-exposure (e∼h), as well as the presence of lens flare (e∼h), moving individuals (i∼k), highly reflective metallic surfaces and glasses (l). These characteristics of the input camera images make the dataset challenging for camera-based SLAM systems.

Section 2: The qualitative results of our reconstructed radiance map on R^{3}LIVE-dataset

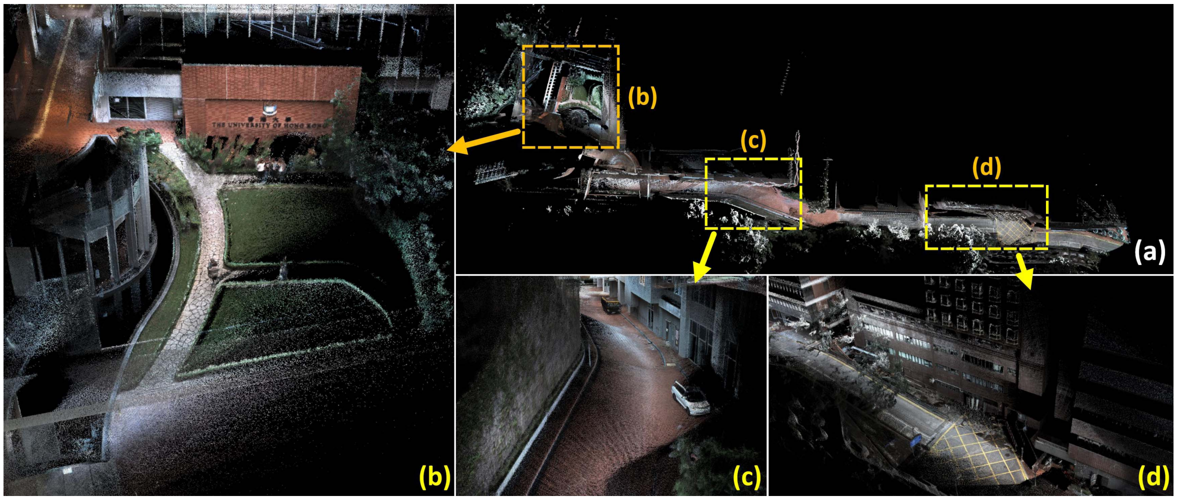

Fig. 3 – Sequence "**hku_campus_seq_01**" is collected by walking along the drive way of the HKU campus. (a) is the birdview of the whole radiance map, with its details shown in (b$\sim$ d).

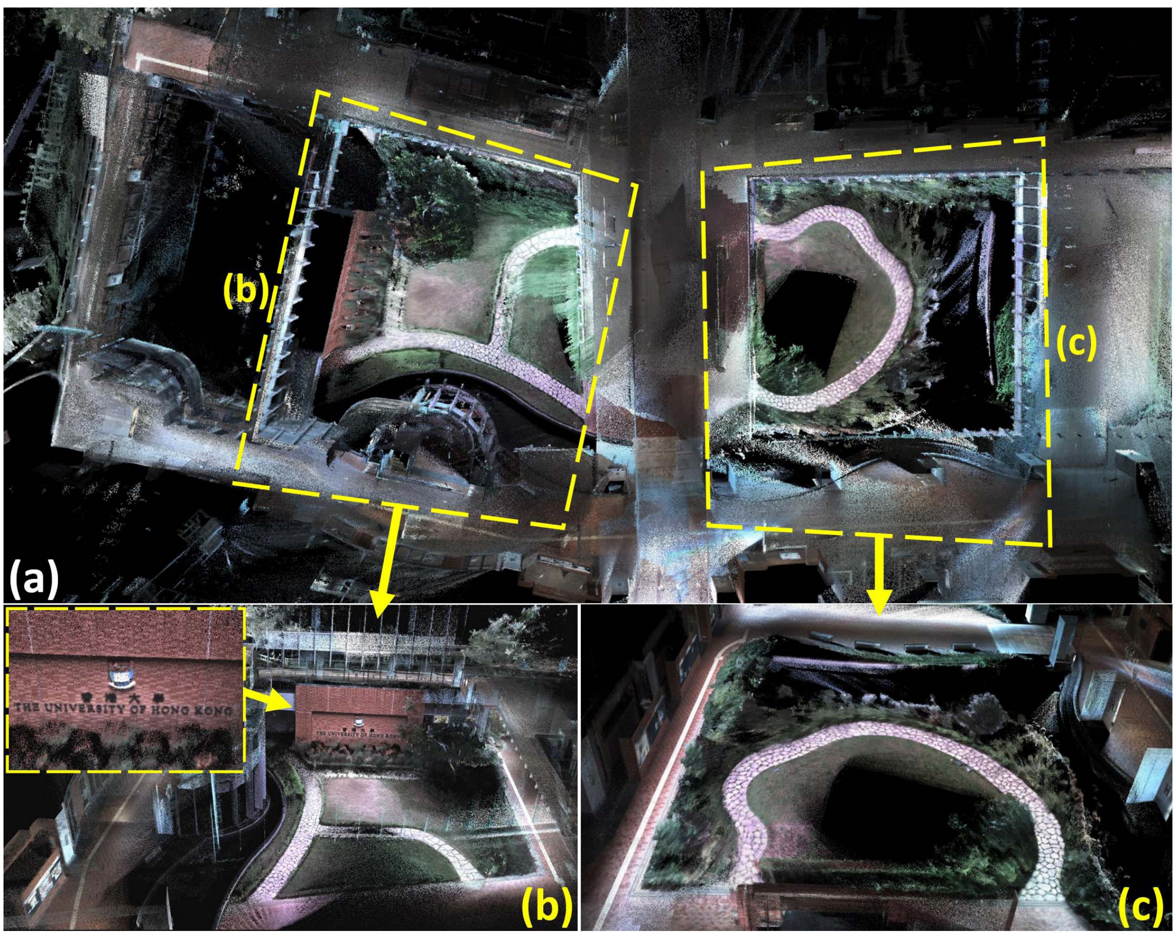

Fig. 4 – Sequence "**hku_campus_seq_00/02/03**" are sampled at the same place but at different times of day (evening, noon and morning, respectively) and with different traveling trajectories. (a) is the birdview of map of sequence "**hku_campus_seq_02**", with the closeup view of details are shown in (b) and (c).

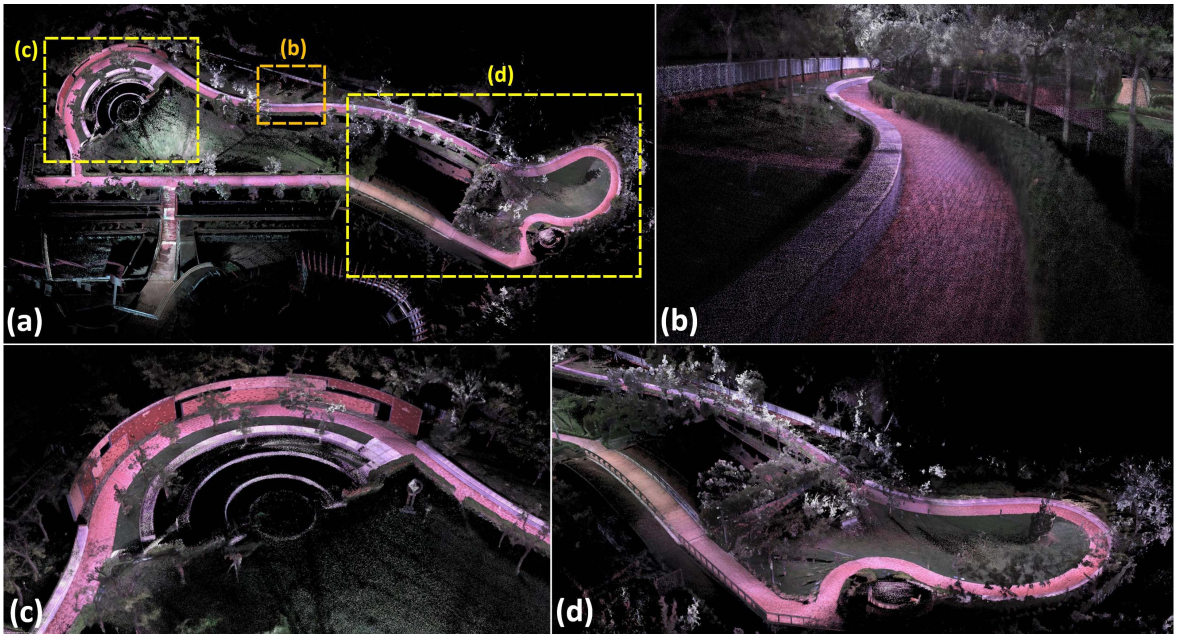

Fig. 5 – Sequence "**hku_park_00**" is collected by walking along the pathway of a garden of HKU. (a) is the birdview of the whole radiance map, with its details shown in (b∼ d).

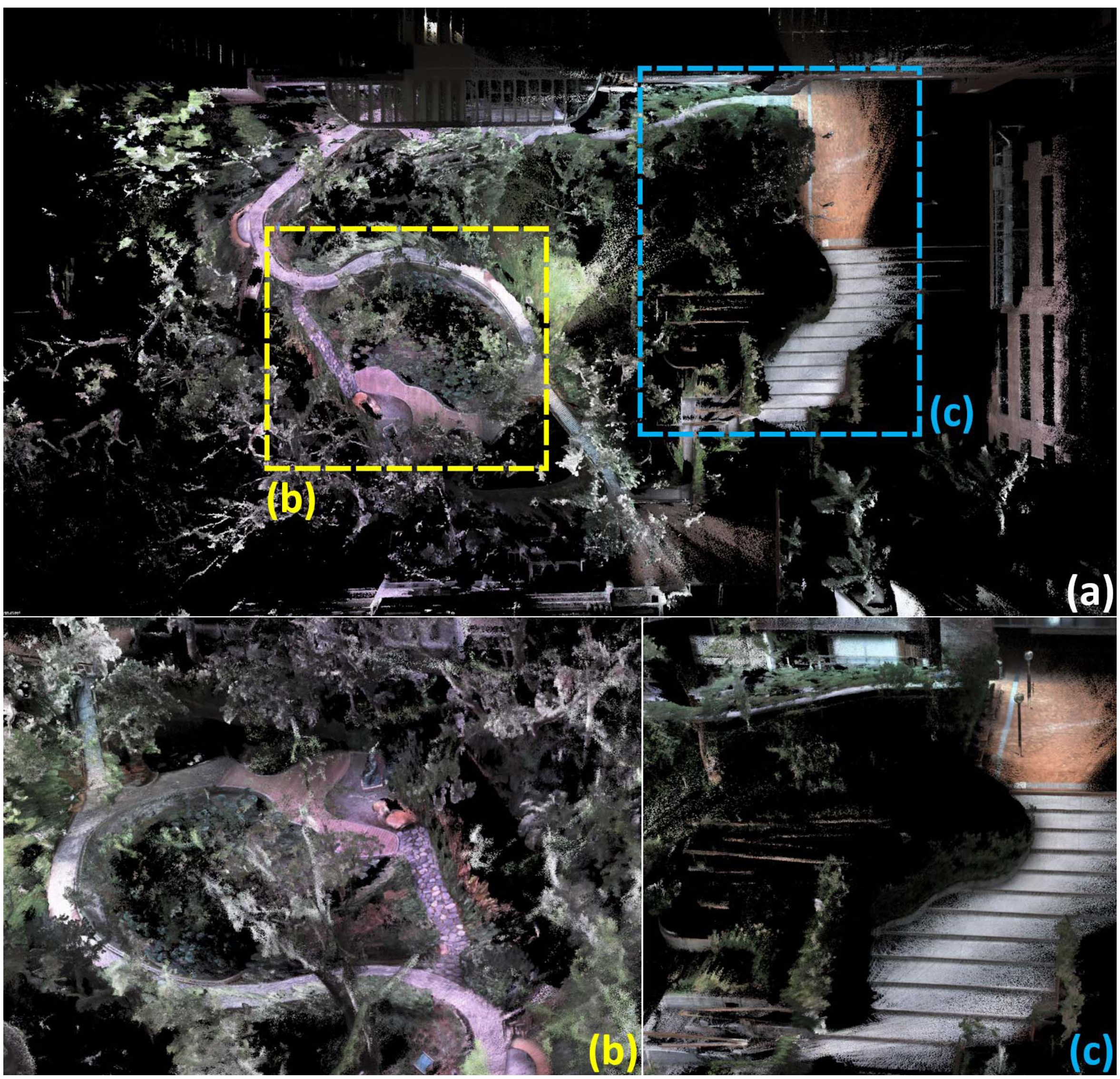

Fig. 6 – Sequence "**hku_park_01**" is collected in a cluttered environment with many trees and bushes. (a) is the birdview of the whole radiance map, with its details are shown in (b) and (c).

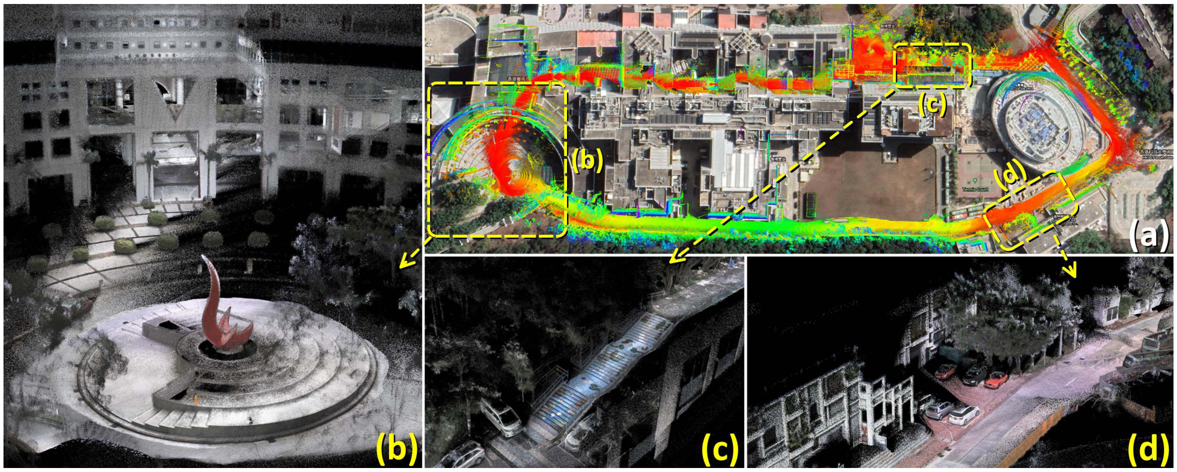

Fig. 7 – Sequence "**hku_campus_seq_00/01**" are collected within the campus of HKUST with two different traveling trajectories. In (a), we merge the point cloud of sequence "**hku_campus_seq_00**" with the GoogleEarth satellite image and find them aligned well. The details of our reconstructed radiance map are selectively shown in (b∼d).

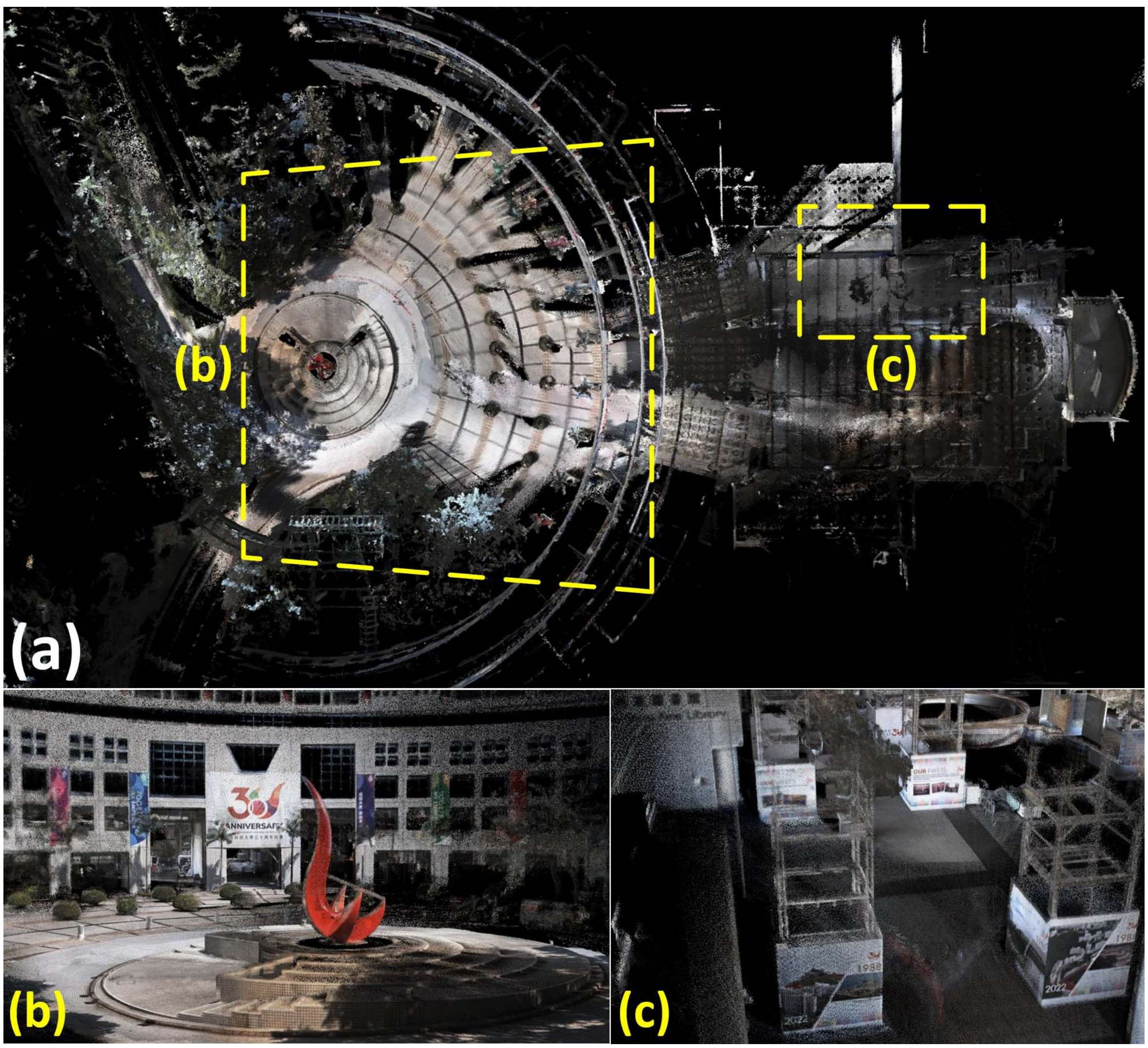

Fig. 8 – Sequence "**hku_campus_seq_02**" is collected by exploring the entrance piazza of HKUST, traveling both the interior and exterior of the buildings. (a) is the birdview of the whole radiance map, with the outdoor and indoor scenarios selectively shown in (b) and (c), respectively.

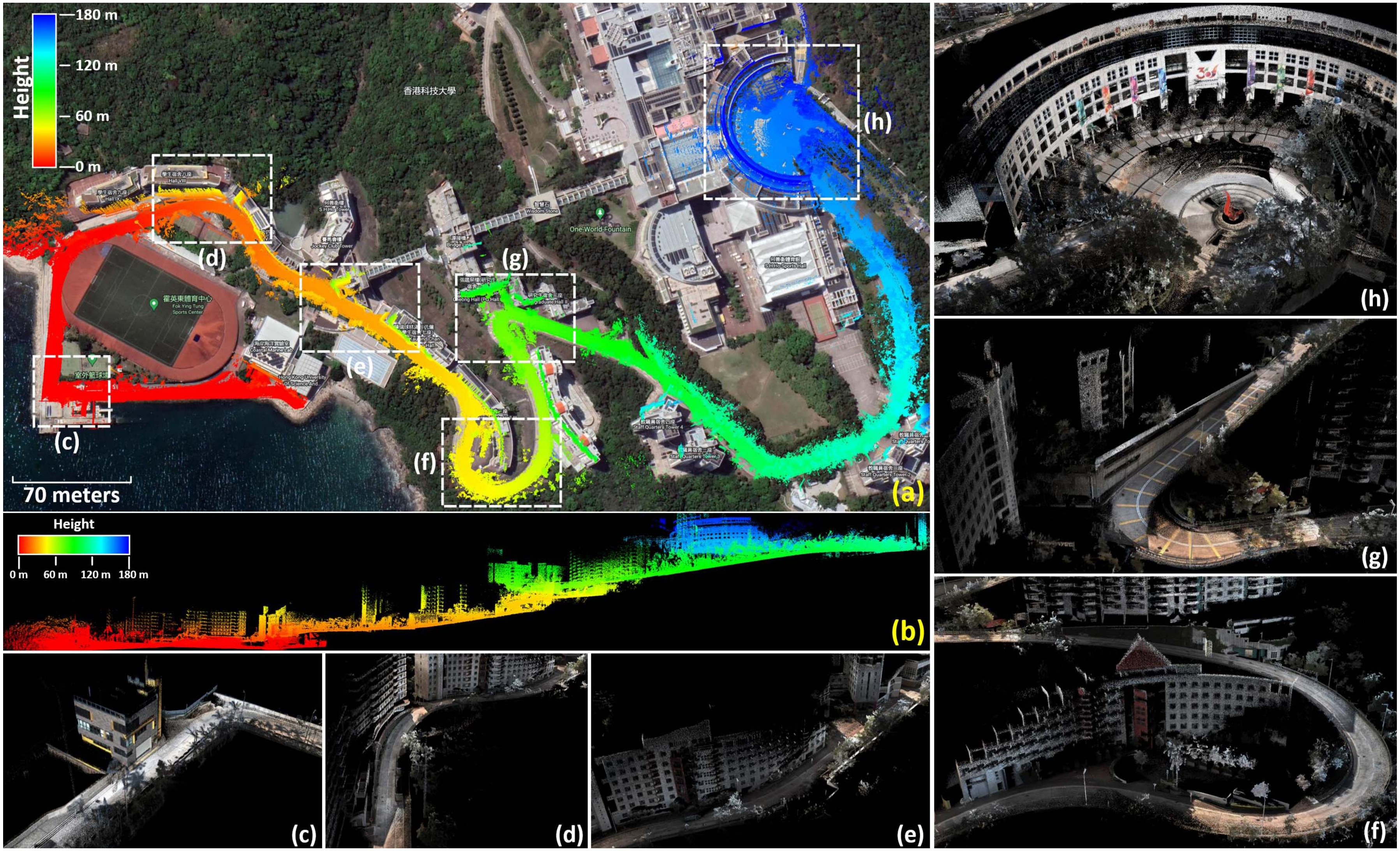

Fig. 9 – Sequence "**hkust_campus_seq_03**" captures most part of the HKUST's campus, with the traveling length reaching 2.1 km. We collected the data starting from the sea front (see the lower left of (a)) and ending at the entrance piazza (the upper right of (a)) of HKUST. In (a), we merge our reconstructed point cloud map (points are colored by their heigh) with the Google Earth satellite image and find them aligned well. (b) shows the side view of the map. (c∼h) are the closeup views of the details marked in (a). To see the real-time reconstruction process of the map, please refer to the video on YouTube: `youtu.be/rpU7wfEtI9w?t=261`.

Section 3: The average time consumption of R^{3}LIVE++ on two datasets

TABLE 1 - The average time consumption per LiDAR or camera frame of our system on NCLT-dataset.

NCLT-dataset Sequence (date)	LiDAR frame Mean $\pm$ STD (ms)	Camera frame Mean $\pm$ STD (ms)
2012-01-08	33.852 $\pm$ 9.110	15.911 $\pm$ 4.180
2012-01-15	35.517 $\pm$ 11.602	17.613 $\pm$ 4.275
2012-01-22	34.392 $\pm$ 11.719	16.551 $\pm$ 4.591
2012-02-02	33.812 $\pm$ 11.188	16.926 $\pm$ 4.361
2012-02-04	32.599 $\pm$ 10.498	15.09 $\pm$ 4.164
2012-02-05	34.823 $\pm$ 11.147	17.09 $\pm$ 4.276
2012-02-12	32.738 $\pm$ 11.765	17.071 $\pm$ 3.846
2012-02-18	37.284 $\pm$ 10.169	17.087 $\pm$ 3.973
2012-02-19	38.004 $\pm$ 9.928	18.179 $\pm$ 4.099
2012-03-17	32.196 $\pm$ 11.154	17.304 $\pm$ 4.370
2012-03-31	36.283 $\pm$ 10.377	16.228 $\pm$ 4.312
2012-04-29	33.652 $\pm$ 9.014	16.487 $\pm$ 4.018
2012-05-11	34.044 $\pm$ 8.964	17.357 $\pm$ 3.811
2012-05-26	37.623 $\pm$ 11.315	15.228 $\pm$ 4.384
2012-06-15	29.07 $\pm$ 8.807	17.254 $\pm$ 3.881
2012-08-04	29.231 $\pm$ 10.427	17.267 $\pm$ 4.629
2012-08-20	28.561 $\pm$ 10.952	15.73 $\pm$ 3.931
2012-09-28	36.692 $\pm$ 10.738	15.458 $\pm$ 4.346
2012-10-28	36.147 $\pm$ 11.497	16.081 $\pm$ 4.102
2012-11-04	37.066 $\pm$ 11.430	16.242 $\pm$ 4.061
2012-11-17	38.153 $\pm$ 9.187	16.931 $\pm$ 3.904
2012-12-01	36.357 $\pm$ 11.660	16.492 $\pm$ 4.165
2013-01-10	32.977 $\pm$ 10.355	18.328 $\pm$ 3.971
2013-02-23	36.171 $\pm$ 10.720	15.368 $\pm$ 4.358
2013-04-05	29.542 $\pm$ 10.052	15.725 $\pm$ 4.189
Average	34.271 $\pm$ 10.551	16.600 $\pm$ 4.168

TABLE 2 - The average time consumption per LiDAR or camera frame of our system on R^{3}LIVE-dataset.

Sequence (date)	LiDAR frame Mean $\pm$ STD (ms)	Camera frame Mean $\pm$ STD (ms)
degenerate_seq_00	17.927 $\pm$ 9.080	13.057 $\pm$ 2.675
degenerate_seq_01	8.111 $\pm$ 3.622	12.111 $\pm$ 2.502
degenerate_seq_02	21.638 $\pm$ 6.793	13.543 $\pm$ 3.014
hku_campus_seq_00	27.659 $\pm$ 8.159	18.829 $\pm$ 3.719
hku_campus_seq_01	25.328 $\pm$ 11.246	18.187 $\pm$ 2.860
hku_campus_seq_02	20.757 $\pm$ 5.109	16.928 $\pm$ 2.518
hku_campus_seq_03	21.705 $\pm$ 4.903	16.040 $\pm$ 2.338
hku_main_building	25.123 $\pm$ 10.246	17.023 $\pm$ 2.512
hku_park_00	26.908 $\pm$ 7.196	17.882 $\pm$ 2.545
hku_park_01	24.412 $\pm$ 6.598	17.479 $\pm$ 2.485
hkust_campus_seq_00	28.160 $\pm$ 9.703	16.624 $\pm$ 2.756
hkust_campus_seq_01	27.058 $\pm$ 10.135	16.138 $\pm$ 2.813
hkust_campus_seq_02	22.857 $\pm$ 6.135	16.518 $\pm$ 2.618
hkust_campus_seq_03	30.757 $\pm$ 5.109	16.928 $\pm$ 2.518
Average	23.453 $\pm$ 7.431	16.234 $\pm$ 2.705

Section 4: R^{3}LIVE++ for Various 3D Applications

Section 4.1: Mesh Reconstruction and Texturing

While R^{3}LIVE++ reconstructs the colored 3D map in real-time, we also develop software utilities to mesh and texture the reconstructed map offline (see Fig. 10). For meshing, we make use of the Delaunay triangulation and graph cuts [2] implemented in CGAL [3] and openMVS [4]. After the mesh construction, we texture the mesh with the vertex (point) colors, with are rendered by our VIO subsystem.

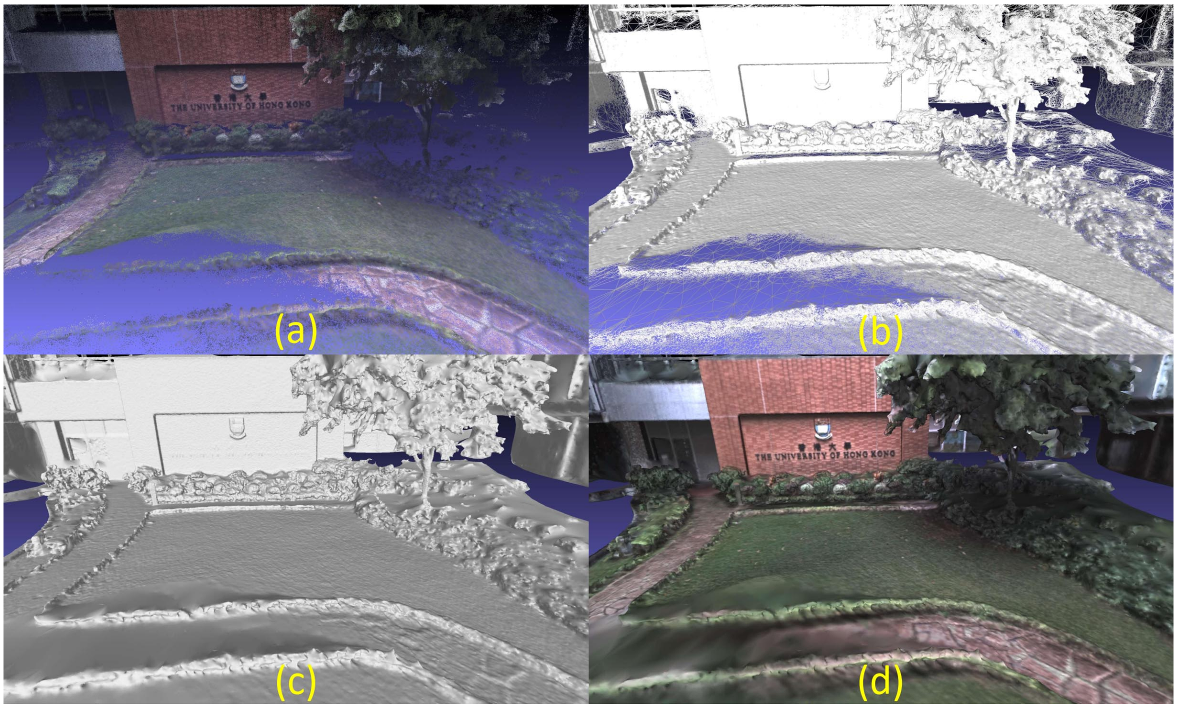

Fig. 10 – (a) show the RGB-colored 3D points reconstructed by R^{3}LIVE++. (b) and (c) show the wireframe and surface of our reconstructed mesh. (d) show the mesh after texture rendering.

Our developed utilities also export the colored point map from R^{3}LIVE++ or the offline meshed map into commonly used file formats such as "pcd", "ply", "obj", etc. As a result, the maps reconstructed by R^{3}LIVE++ can be imported into various 3D software, including but not limited to CloudCompare [5], Meshlab [6], AutoDesk 3ds Max [7].

Section 4.2: Mesh Reconstruction and Texturing

With the developed software utilities, we can export the reconstructed 3D maps to Unreal Engine [8] to enable a series of 3D applications. For example, in Fig. 11(a), we built a car simulator with the AirSim [9]. In Fig. 11(b) and Fig. 11(c), we used our reconstructed maps to develop video games for mobile platforms and desktop PCs, respectively. To get more details about our demos, we refer the readers to watch our video on YouTube: `youtu.be/39YKzG7K0w0`.

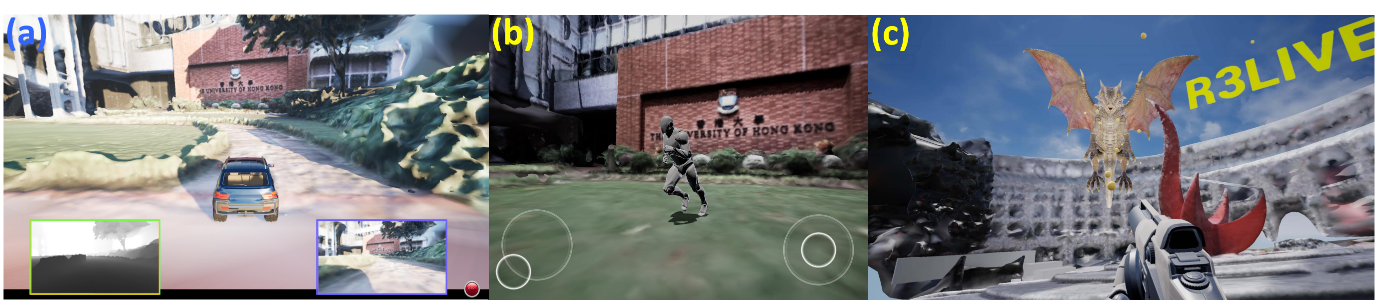

Fig. 11 – In (a), we built a car simulator with our maps and AirSim. The images in yellow and blue frame-boxes are the depth and RGB image query from the AirSim's API. In (b) and (c), we developed video games for mobile platforms and desktop PCs. The player in (b) is controlling the actor to explore the campus of HKU, and in (c) is fighting against a dragon by shooting rubber balls at HKUST.

REFERENCES

[1] W. Sun, Y. Hu, D. G. MacDonnell, C. Weimer, and R. R. Baize, "Technique to separate lidar signal and sunlight," *Optics express*, vol. 24, no. 12, pp. 12 949–12 954, 2016.

[2] P. Labatut, J.-P. Pons, and R. Keriven, "Efficient multi-view reconstruction of large-scale scenes using interest points, delaunay triangulation and graph cuts," in *2007 IEEE 11th international conference on computer vision*. IEEE, 2007, pp. 1–8.

[3] A. Fabri and S. Pion, "Cgal: The computational geometry algorithms library," in *Proceedings of the 17th ACM SIGSPATIAL international conference on advances in geographic information systems*, 2009, pp. 538–539. [Online]. Available: https://www.cgal.org

[4] D. Cernea, "OpenMVS: Multi-view stereo reconstruction library," 2020. [Online]. Available: https://cdcseacave.github.io/openMVS

[5] D. Girardeau-Montaut, "Cloudcompare," *France: EDF R&D Telecom ParisTech*, 2016. [Online]. Available: https://www.danielgm.net/cc

[6] P. Cignoni, G. Ranzuglia, M. Callieri, M. Corsini, F. Ganovelli, N. Pietroni, and M. Tarini, "Meshlab," 2011. [Online]. Available: https://www.meshlab.net

[7] Autodesk, "Autodesk 3ds max." [Online]. Available: https://www.autodesk.com/products/3ds-max

[8] Epic Games, "Unreal engine." [Online]. Available: https://www.unrealengine.com

[9] S. Shah, D. Dey, C. Lovett, and A. Kapoor, "Airsim: High-fidelity visual and physical simulation for autonomous vehicles," in *Field and service robotics*. Springer, 2018, pp. 621–635. [Online]. Available: https://microsoft.github.io/AirSim